Realization of All-Optical Discrete Cosine and Sine Transforms Using MMI Structures on an SOI platform

[1]Trung-Thanh Le, [2]Laurence Cahill

[1]Hanoi University of Natural Resources and Environment
41A, K1 Road, Tu Liem, Hanoi, Vietnam
[2]La Trobe University, Melbourne, Vic 3086, Australia

ABSTRACT

The Discrete Cosine Transform (DCT) and Discrete Sine Transform (DST) have found applications in digital signal, image and video processing and particularly in transform coding systems for data compression and decompression. Multimode interference (MMI) in optical silicon on insulator (SOI) waveguides is attractive for realizing all-optical DCT and DST transforms as they have the advantages of low loss, ultra-compact size and excellent fabrication tolerances. In this paper, a novel approach to realize all-optical type I, II, III and IV DCT and DST based on multimode interference structures on silicon on insulator platform is proposed. Based on the transfer matrix method, the analytical expressions describing the characteristics of the MMI structures are derived. Designs of the proposed devices are then verified and optimized using 2D and 3D BPM simulations.

Key words: *Multimode interference, optical logic, optical Fuzzy logic, optical signal processing, optical transformations.*

1. INTRODUCTION

For many years, optical techniques have been considered for a variety of signal processing tasks such as pattern recognition, the generation of ambiguity surfaces for radar signal processing and image processing applications [1, 2]. The major reason for using an optical signal processor is its high bandwidth advantage over electronic processors. Due to its high throughput, the application of optical signal processing in optical communication systems is a very attractive research area. Photonic signal processing transforms such as the discrete Fourier transform (DFT), discrete cosine transforms (DCT) and discrete wavelet transforms (DWT) are useful for spatial signal processing and optical computing such as spectrum analysis, filtering, and encoding, etc.

Early efforts used lens systems [3, 4], directional couplers [5, 6], and single mode star networks [7] to develop optical signal processing transforms such as the Hadamard transform, the DFT and wavelet filters. However, the systems based on these technologies are usually quite large, lack accuracy and require high precision mechanical placement. In addition, the structure for implementing the transforms based on fibre technology requires bulky crossovers of fibre cables. Recently, the design of DFT and DCT transforms using fibre directional couplers has been presented by Moreolo and Cincotti [8]. In the literature [9, 10], a few transforms such as Hadamard transforms and discrete unitary transformations have employed MMI structures and multimode waveguide holograms. However, these devices were designed for the InP material system. For the device using holograms, a complex fabrication process is required. The presence of holograms within the multimode waveguide tends to introduce additional losses.

Recently, a method for realizing all-optical Fourier transform based on multimode interference has been reported [11]. The design of these devices has been implemented on the silica material system. In this paper, we propose a new method to realize all-optical discrete cosine transform (DCT) and all-optical discrete sine transform (DST) type I, II, III and IV based on multimode interference (MMI) structures using silicon waveguides.

Recently, the realization of all-optical Fourier transform and discrete Haar transforms based on multimode interference has been presented [11-13]. The design of these devices has been implemented on the silica material system. Due to the low index contrast of the material system, the size of the realized devices is large and it is not suitable to photonic integrated circuits. In addition, the realization of the type I, II, III and IV DCT and DST (DCT-I, II, III, IV and DST-I, II, III, IV), which is suitable for photonic integrated circuits, has not been reported. Therefore, in this paper, we propose a new method to realize all-optical DCT/DST-I, II, III, IV transforms based on multimode interference (MMI) structures using silicon waveguides. Both DCT and DST transforms are realized on the same device structure. Multimode interference couplers have found in many optical the desirable advantages of low loss, compactness and good fabrication tolerances [14]. In addition, the available material systems used for such multimode devices include polymers, silica on silicon and silicon-on-insulator (SOI). The high-index contrast silicon-on-insulator (SOI) platform has attracted much interest due to its potential for miniaturization,

improved performance, and compatibility with existing CMOS technology [15].

The proposed devices are analyzed and optimized using the transfer matrix method and the beam propagation method (BPM) [16]. A description of the general theory behind the use of multimode structures to achieve the DCT and DST device presented in Section 2. Simulation results of MMI based structures for components in the device structure are covered in Section 3. A brief summary of the results of this research is given in Section 4.

2. PRINCIPLE OF OPERATION

In this section, we show the general theory for realizing the DCT and DST transforms using MMI structures. The transfer matrix method is used to derive the analytical expressions of the DCT and DST matrices.

2.1 Optical Type-IV Discrete Cosine and Sine Transforms (DCT-IV & DST-IV)

The MMI coupler has a structure consisting of a homogeneous planar multimode waveguide region connected to a number of single mode access waveguides. The operation of optical MMI coupler is based on the self-imaging principle [14, 15]. Self-imaging is a property of a multimode waveguide by which as input field is reproduced in single or multiple images at periodic intervals along the propagation direction of the waveguide. The central structure of the MMI filter is formed by a waveguide designed to support a large number of modes.

In this paper, the access waveguides are identical single mode waveguides with width W_a. The input and output waveguides are located at

$$x = (i + \frac{1}{2})\frac{W_{MMI}}{N} \ , \ (i=0,2,\ldots,N\text{-}1) \tag{1}$$

The electrical field inside the MMI coupler can be expressed by [17]

$$E(x,z) = e^{-jkz} \sum_{m=1}^{M} E_m \exp(j\frac{m^2\pi}{4\Lambda}z)\sin(\frac{m\pi}{W_{MMI}}x) \tag{2}$$

where $k = 2\pi n / \lambda$, λ is the operating wavelength, n is the waveguide refractive index and M is the total number of guided modes in the MMI coupler, E_m is the summation coefficients. We have the orthogonal set relating the internal modes field to the outer input-output field

$$V_{ir} = \begin{cases} \sqrt{\frac{2}{N}}\ sin(\frac{r\pi}{N}(i+\frac{1}{2})) & (r \neq N) \\ \\ \sqrt{\frac{2}{N}}\ sin(\pi(i+\frac{1}{2})) & (r = N) \end{cases} \tag{3}$$

where V_{ir} is the element on row i and column r of a matrix $\mathbf{V_N}$, which relates the propagation modes inside the waveguide to the output field.

It is assumed that the length of the MMI coupler is set to $L_{MMI} = 2\Lambda / N$, where $\Lambda = nW_{MMI}^2 / \lambda$. If the common phase term in equation (2) is not considered, the *ith* propagating modes will experience different phase shift of $i^2\pi / (2N)$ and the matrix $\mathbf{V_N^T}$ is then multiplied by a diagonal matrix with the diagonal elements [9]

$$b_{rr} = \exp(j\frac{r^2\pi}{2N}) \tag{4}$$

The total transfer matrix of the waveguide from input to the output ports now can be calculated by

$$\mathbf{M} = \mathbf{VBV^T} \tag{5}$$

This equation can be rewritten by

$$M_{uv} = je^{j\frac{\pi}{4}}\sqrt{\frac{2}{N}}\ sin(\frac{\pi(u+\frac{1}{2})(v+\frac{1}{2})}{N})e^{(-j\pi\frac{(u+\frac{1}{2})^2+(v+\frac{1}{2})^2}{2N})} \tag{6}$$

If the phase shifters are added to the input ports and output ports of the MMI structure, the total transfer matrix can be calculated by

$$\mathbf{T} = \mathbf{D_{out}MD_{in}} \tag{7}$$

Where $\mathbf{D_{in}}$ and $\mathbf{D_{out}}$ are the matrices indicating the contribution of the input and output phase shifters arrays. If the phase shifter are set to be $\pi(i+\frac{1}{2})^2 / (2N)$, i=0, 2,…,N-1, at the input and output waveguides, the total transfer matrix T can be computed by

$$T_{uv} = je^{j\frac{\pi}{4}}\sqrt{\frac{2}{N}}\ sin(\frac{\pi(u+\frac{1}{2})(v+\frac{1}{2})}{N}) \tag{8}$$

In addition, the DST-IV can be described by the matrix

$$M_{DST} = \sqrt{\frac{2}{N}}\ sin(\frac{\pi(u+\frac{1}{2})(v+\frac{1}{2})}{N}) \tag{9}$$

Therefore, the matrix of equation (8) is the matrix of the type IV DST (DST-IV) if the phase factor $jexp(j\frac{\pi}{4})$ is neglected.

Also, the matrix of the type IV DCT (DCT-IV) can be expressed by

$$M_{DCT} = \sqrt{\frac{2}{N}} \cos(\frac{\pi(u+\frac{1}{2})(v+\frac{1}{2})}{N}) \qquad (10)$$

It is can be proved that $\mathbf{M_{DCT} = PM_{DST}Q}$, where

$$\mathbf{P} = \begin{pmatrix} & & & & 1 \\ & & & 1 & \\ & & .. & & \\ & 1 & & & \\ 1 & & & & \end{pmatrix}, \mathbf{Q} = \begin{pmatrix} 1 & & & & \\ & -1 & & & \\ & & 1 & & \\ & & & -1 & \\ & & & & .. \end{pmatrix} \qquad (11)$$

Therefore, the DCT-IV can be implemented using the DST–IV device based on MMI structures by putting a phase shifter π at the even input ports and re-labeling all the output ports with the inverse order.

2.2 Optical Type-I Discrete Cosine and Sine Transforms (DCT-I and DST-I)

The DCT-I of an input sequence $\{x_n\}\big|_{n=0,..,N-1}$ is given by [18]

$$y_k = \sum_{n=0}^{N-1} \sqrt{\frac{2}{N}} x_n \cos(\frac{\pi}{N}nk) \qquad (11)$$

where k= 0, 1,…,N-1. The DST-I of an input sequence $\{x_n\}\big|_{n=0,..,N-1}$ is given by

$$y'_k = \sum_{n=0}^{N-1} \sqrt{\frac{2}{N}} x_n \sin(\frac{\pi}{N}nk) \qquad (12)$$

We can rewrite the factor within the cosine and sine functions by

$$\frac{\pi}{N}nk = \frac{\pi}{N}(n+\frac{1}{2})(k+\frac{1}{2}) - \frac{\pi}{N}(\frac{n}{2}+\frac{k}{2}+\frac{1}{4}) \qquad (13)$$

As a result, the DCT-I and DST-I transforms can be achieved simultaneously by using the structure as shown in Fig. 1.

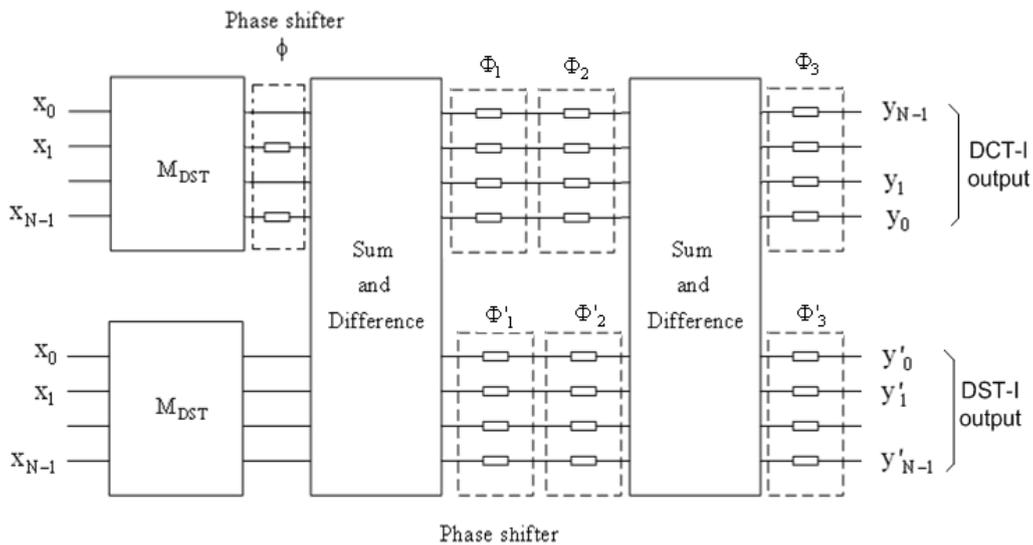**Fig 1. The structure of the DCT-I and DST-I transform**

Where the matrix of the phase shifters ϕ, which is a NxN matrix, must be

$$\phi = \begin{pmatrix} 1 & 0 & ... & 0 \\ 0 & \exp(j\pi) & ... & 0 \\ 0 & 0 & 1 & ... \\ 0 & 0 & ... & \exp(j\pi) \end{pmatrix}_{NxN} \qquad (14)$$

The output signals of the DCT-IV and DST-IV transforms are then put to the input ports of a sum and difference unit (SD unit). The output signals of the sum and difference unit are the sum and difference of its input signals. The transfer matrix of the sum and difference SD is a 2Nx2N matrix and can be expressed by

$$SD = \begin{pmatrix} e^{j\frac{\pi}{4}} & 0 & ... & 0 & e^{j\frac{3\pi}{4}} \\ 0 & e^{j\frac{\pi}{4}} & ... & e^{j\frac{3\pi}{4}} & 0 \\ ... & ... & ... & ... & ... \\ 0 & e^{j\frac{3\pi}{4}} & ... & e^{j\frac{\pi}{4}} & 0 \\ e^{j\frac{3\pi}{4}} & 0 & ... & 0 & e^{j\frac{\pi}{4}} \end{pmatrix}_{2N \times 2N} \quad (15)$$

It can be proved that the phase shifters added to the input and output can be calculated by:

$$\Phi_1 = \begin{pmatrix} e^{-j\frac{\pi}{4}} & 0 & ... & 0 \\ 0 & e^{-j\frac{\pi}{4}} & ... & 0 \\ ... & ... & ... & ... \\ 0 & 0 & ... & e^{-j\frac{\pi}{4}} \end{pmatrix}_{N \times N} , \quad \Phi'_1 = \begin{pmatrix} e^{-j0.75\pi} & 0 & ... & 0 \\ 0 & e^{-j0.75\pi} & ... & 0 \\ ... & ... & ... & ... \\ 0 & 0 & ... & e^{-j0.75\pi} \end{pmatrix}_{N \times N} \quad (16)$$

$$\Phi_2 = \begin{pmatrix} e^{-j\frac{\pi}{N}(\frac{0}{2}+\frac{1}{8})} & 0 & ... & 0 \\ 0 & e^{-j\frac{\pi}{N}(\frac{1}{2}+\frac{1}{8})} & ... & 0 \\ ... & ... & ... & ... \\ 0 & 0 & ... & e^{-j\frac{\pi}{N}(\frac{N-1}{2}+\frac{1}{8})} \end{pmatrix}_{N \times N} , \quad \Phi'_2 = e^{-j0.5\pi} \begin{pmatrix} e^{j\frac{\pi}{N}(\frac{0}{2}+\frac{1}{8})} & 0 & ... & 0 \\ 0 & e^{j\frac{\pi}{N}(\frac{1}{2}+\frac{1}{8})} & ... & 0 \\ ... & ... & ... & ... \\ 0 & 0 & ... & e^{j\frac{\pi}{N}(\frac{N-1}{2}+\frac{1}{8})} \end{pmatrix}_{N \times N} \quad (17)$$

$$\Phi_3 = e^{-j\frac{\pi}{4}} \begin{pmatrix} e^{-j\frac{\pi}{N}(\frac{0}{2}+\frac{1}{8})} & 0 & ... & 0 \\ 0 & e^{-j\frac{\pi}{N}(\frac{1}{2}+\frac{1}{8})} & ... & 0 \\ ... & ... & ... & ... \\ 0 & 0 & ... & e^{-j\frac{\pi}{N}(\frac{N-1}{2}+\frac{1}{8})} \end{pmatrix}_{N \times N} \quad \Phi'_3 = e^{-j0.75\pi} \begin{pmatrix} e^{j\frac{\pi}{N}(\frac{0}{2}+\frac{1}{8})} & 0 & ... & 0 \\ 0 & e^{j\frac{\pi}{N}(\frac{1}{2}+\frac{1}{8})} & ... & 0 \\ ... & ... & ... & ... \\ 0 & 0 & ... & e^{j\frac{\pi}{N}(\frac{N-1}{2}+\frac{1}{8})} \end{pmatrix}_{N \times N} \quad (18)$$

2.3 Optical Type-II Discrete Cosine and Sine Transforms (DCT-II and DST-II)

The DCT-II of an input sequence $\{x_n\}\big|_{n=0,..,N-1}$ is given by [18]

$$y_k = \sum_{n=0}^{N-1} \sqrt{\frac{2}{N}} x_n \cos[(\frac{\pi}{N}n)(k+\frac{1}{2})] \quad (19)$$

where k= 0, 1,…,N-1. The DST-II of an input sequence $\{x_n\}\big|_{n=0,..,N-1}$ is given by

$$y'_k = \sum_{n=0}^{N-1} \sqrt{\frac{2}{N}} x_n \sin[(\frac{\pi}{N}n)(k+\frac{1}{2})] \quad (20)$$

We can rewrite the factor within the cosine and sine functions by

$$[(\frac{\pi}{N}n)(k+\frac{1}{2})] = \frac{\pi}{N}(n+\frac{1}{2})(k+\frac{1}{2}) - \frac{\pi}{N}(\frac{n}{2}+\frac{1}{4}) \quad (13)$$

It is similar to the structure of the DCT-I and DST-I, the DCT-II and DST-II transforms can be achieved simultaneously by using the MMI structure, but the phase shifters are $-\frac{\pi}{N}(\frac{n}{2}+\frac{1}{4})$ for the DCT-II and DST-II at the

input ports, instead of $\frac{\pi}{N}(\frac{n}{2}+\frac{k}{2}+\frac{1}{4})$ at the both input and output ports for the DCT-I and DST-I.

2.4 Optical Type-III Discrete Cosine and Sine Transforms (DCT-III & DST-III)

The DCT-III of an input sequence $\{x_n\}|_{n=0,..,N-1}$ is given by [18]

$$y_k = \sum_{n=0}^{N-1} \sqrt{\frac{2}{N}} x_n \cos[(\frac{\pi}{N}k)(n+\frac{1}{2})] \qquad (19)$$

where k= 0, 1,…,N-1. The DST-III of an input sequence $\{x_n\}|_{n=0,..,N-1}$ is given by

$$y'_k = \sum_{n=0}^{N-1} \sqrt{\frac{2}{N}} x_n \sin[(\frac{\pi}{N}k)(n+\frac{1}{2})] \qquad (20)$$

We can rewrite the factor within the cosine and sine functions by

$$[(\frac{\pi}{N}k)(n+\frac{1}{2})] = \frac{\pi}{N}(n+\frac{1}{2})(k+\frac{1}{2}) - \frac{\pi}{N}(\frac{k}{2}+\frac{1}{4}) \qquad (13)$$

It is similar to the structure of the DCT-I and DST-I, the DCT-II and DST-II transforms can be achieved simultaneously by using the MMI structure, but the phase shifters are $-\frac{\pi}{N}(\frac{k}{2}+\frac{1}{4})$ for the DCT-II and DST-II at the output ports, instead of $\frac{\pi}{N}(\frac{n}{2}+\frac{k}{2}+\frac{1}{4})$ at the both input and output ports for the DCT-I and DST-I.

3. SIMULATION RESULTS AND DISCUSSIONS

The waveguide structure used in the designs is shown in Fig. 2. Here, SiO_2 (n_{SiO_2} =1.46) is used as the upper cladding material. An upper cladding region is needed for devices using the thermo-optic effect in order to reduce loss due to metal electrodes. Also, the upper cladding region is used to avoid the influence of moisture and environmental temperature [19].
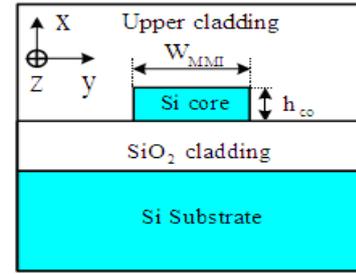

Fig 2. Silicon waveguide cross-section used in the designs of the proposed device

The parameters used in the designs are as follows: the waveguide has a standard silicon thickness of $h_{co} = 220$nm and access waveguide widths are $W_a = 0.5$ μm for single mode operation and low loss [20]. It is assumed that the designs are for the transverse electric (TE) polarization at a central optical wavelength $\lambda = 1550$nm. In this study, we use the three dimensional beam propagation method (3D-BPM) to design the units used in the whole structure [21]. Because it is a time-consuming process if the whole structure is investigated using the 3D-BPM, the BPM simulation will be used to verify the principle of operation of the units as follows.

3.1 Simulation of the DCT-IV and DST-IV

The DCT-IV and DST-IV (N-point) can be achieved by using an NxN MMI coupler. Simulations of the whole device are a time consuming process. Without loss of generality, each part of the whole device will be investigated independently. First, the design of all optical 4 point DCT and DST is carried out in this study.

The width and the length of the 4x4 MMI coupler used for designing the 4 point DCT-IV and DST-IV need to be carefully chosen. By using the 3D-BPM simulation, the optimal width of the MMI coupler is to be W_{MMI} =4μm for compactness and low loss. In addition, the access waveguide is tapered to a width of $W_{tp} = 800$nm to improve device performance [22]. The optimized length of the MMI coupler calculated by using 3D-BPM is $L_{MMI} = 16.2$ μm. As an example, we assume that the input vector is to be $(x_0 x_1 x_2 x_3)^T = (1100)^T$ and the all-optical DST-IV is performed. The normalized input and output amplitudes are shown in Fig. 3(a) and 3(b), respectively. The 3D BPM simulation for this case is shown in Fig. 3(c).

(a)   (b)   (c)
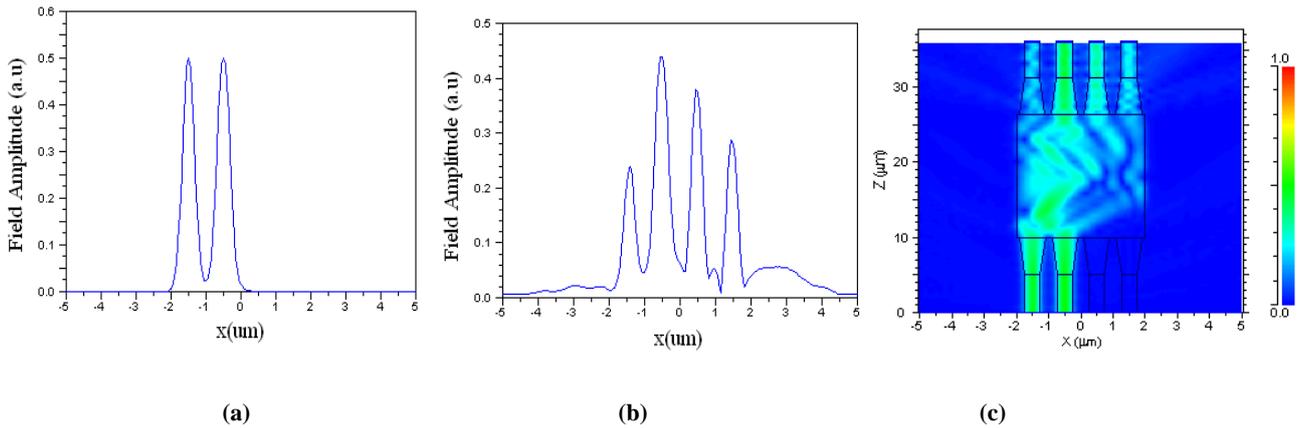
Fig 3. BPM simulation result of the DST-IV transform: (a) input amplitude for input vector $(1100)^T$, (b) output amplitude and (c) field propagation; the all-optical DCT-IV is performed

It is obvious from the simulations that the BPM simulation results have a good agreement with the prediction of the theory.

3.2 Simulation of the Sum and Difference Unit

We have shown previously that the transfer matrix of the sum and difference (SD) unit given by (15) can be realized by using an NxN MMI structure [22]. As an example, for N=8, the matrix of the SD unit can be achieved if the length of an 8x8 MMI coupler is to be $L_{MMI} = \dfrac{3L_\pi}{2}$,

where $L_\pi = \dfrac{4}{3}\Lambda$ is the beat length of the MMI coupler. Figure 3 shows the SD unit based on an 8x8 MMI coupler, where the width of the MMI coupler is W_{MMI} and the separation between two adjacent parallel waveguides is $W_{MMI}/8$.
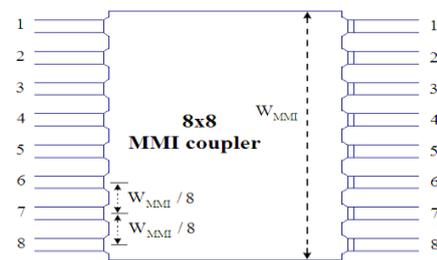

Fig 3. Sum and difference (SD) unit based on an 8x8 MMI coupler

We will show that the sum and difference unit can be realized using 8x8 MMI structures if the width and length of the MMI coupler are chosen properly. We choose an 8x8 MMI coupler having a width of $W_{MMI} = 9\mu m$. The 3D-BPM simulations for optimized designs of 8x8 MMI structures based on the silicon waveguide having a width of $W_{MMI} = 9\mu m$ are shown in Fig. 4. The optimized length calculated to be $L_{MMI} \approx 382\mu m$. Fig. 4(a) and (b) show the field propagation through the SD unit for input signals presented at input port 1, 8 and at ports 2, 7, respectively
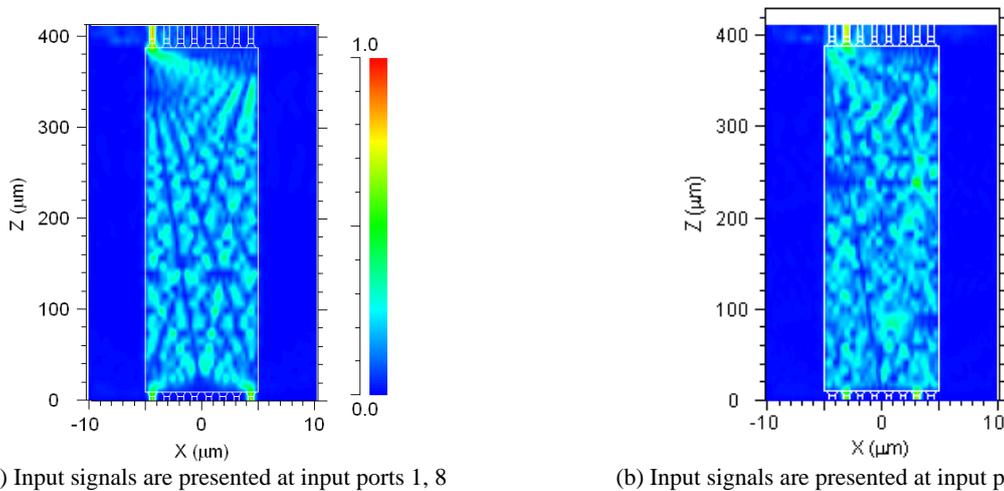

(a) Input signals are presented at input ports 1, 8   (b) Input signals are presented at input ports 2, 7

Fig 4. BPM simulation result for the field propagation within the sum and difference unit using an 8x8 MMI structure.

41

The simulations show that the sum of the two signals can be obtained at output port 8 and the difference of the two signals can be obtained at output port 1.

3.3 Realization of the Phase Shifter in the Silicon Nanowire Waveguides

The phase shifters incorporated with the MMI structures are particularly important to realize the appropriate functions of all-optical DCT and DST transforms. It is possible to realize an optical phase shifter by using a curved waveguide section, a wide waveguide, a multimode waveguide, a special patterned waveguide or a heated waveguide based on the thermo-optic effect [22]. Here, we investigate the approach for implementing the phase shifters by using the multimode waveguides [23] due to their advantages of small size, low loss and ease of fabrication with the existing CMOS technology.

The multimode section can be viewed as a 1x1 SI-MMI coupler and the symmetric interference (SI) theory [15] can be used to determine the length L_M to give a single self-image at the end of the section. The width of the multimode silicon waveguide section is chosen to be in the range $1\mu m$ to $2\mu m$ in order to support at least three guided modes. It therefore acts as a small MMI coupler. The overall size of the device is not increased significantly. The length of the phase shifter is chosen to form a single-image at the output. If there are two adjacent waveguides and an additional phase shift is required for one waveguide, then a small MMI with tapered input and output sections can be used as shown in Fig. 5(a). This figure also shows the 3D-BPM simulation for the fields propagating through a multimode waveguide section having a width of $1.5\mu m$ and through a single mode waveguide as an example. The tapered waveguides are used to reduce losses in this design. The phase shift due to the MMI taper is compensated by inserting a taper into the other waveguide. In practice, the single mode waveguide would not have a tapered section. The phase shift which can be achieved using different widths and optimized lengths of the multimode waveguide section is shown in Fig. 5(b). It can be seen from this diagram that a particular phase shift can be achieved simply by appropriately choosing the width and length of the multimode waveguide section.
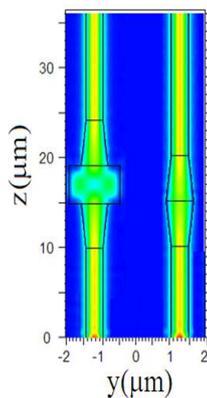
(a) Field propagation
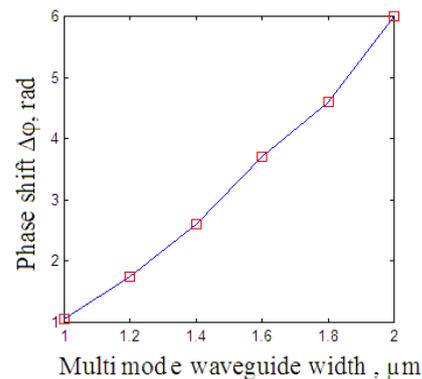
(b) Induced phase shift

Fig. 6 Phase shift made by using a multimode section (a) the field propagation through a 1x1 multimode waveguide having a width of $1.5\mu m$ compared to a single mode waveguide and (b) phase shifts at different multimode waveguide widths

In summary, it is obvious from the 3D-BPM simulation results that the theory predicts accurately the field propagation in the devices. By cascading the MMI structures which have been used for the DCT-IV, DST-IV, sum and difference unit along with the phase shifters, the whole DCT-I, II, III and DST-I, II, III transforms can be achieved.

4. CONCLUSION

We have proposed a new method for realizing all-optical DCT-I, II, III, IV and DST-I, II, III, IV transforms using multimode interference structures on an SOI platform. The designs of the proposed devices have been carried out using the transfer matrix method and the beam propagation method.

REFERENCES

[1] VanderLugt, Optical signal processing. New York: J. Wiley & Sons, 1992.

[2] N. B. Le, *Photonic signal processing : techniques and applications*: CRC Press, 2007.

[3] J. W. Goodman, A. R. Dias, and L. M. Woody, "Fully parallel, high-speed incoherent optical method for performing discrete Fourier transforms," *Optics Letters*, vol. 2, pp. 1-3, 1978.

[4] D. G. Sun, N. X. Wang, and L. M. H. e. al., "Butterfly interconnection networks and their applications in information processing and optical computing:

42

applications in fast-Fourier-transform-based opticalinformation processing," *Applied Optics*, vol. 32, pp. 7184-7193, 1993.

[5] A. E. Siegman, "Fiber Fourier optics," *Optics Letters*, vol. 26, pp. 1215-1217, 2001.

[6] G. Cincotti, "Fiber wavelet filters," *IEEE Journal of Quantum Electronics*, vol. 38, pp. 1420-1427, 2002.

[7] M. E. Marhic, "Discrete Fourier transforms by single-mode star networks," *Optics Letters*, vol. 12, pp. 63-65, 1987.

[8] M. S. Moreolo and G. Cincotti, "Fiber optics transforms," presented at 10th Anniversary International Conference onTransparent Optical Networks (ICTON 2008), Athens. Greece, 22-26 June 2008.

[9] A. R. Gupta, K. Tsutsumi, and J. Nakayama, "Synthesis of Hadamard Transformers by Use of Multimode Interference Optical Waveguides," *Applied Optics*, vol. 42, pp. 2730-2738, 2003.

[10] S. Tseng, Y. Kim, C. J. K. Richardson, and J. Goldhar, "Implementation of discrete unitary transformations by multimode waveguide holograms," *Applied Optics*, vol. 45, pp. 4864-4872 2006.

[11] J. Zhou, "Realization of Discrete Fourier Transform and Inverse Discrete Fourier Transform on One Single Multimode Interference Coupler," *IEEE Photonics Technology Letters*, vol. 23, pp. 302 - 304, 2011.

[12] J. Zhou and M. Zhang, "All-Optical Discrete Sine Transform and Discrete Cosine Transform Based on Multimode Interference Couplers," *IEEE Photonics Technology Letters*, vol. 22, pp. 317 - 319, 2010.

[13] T.-T. Le, "The Design of Optical Signal Transforms Based on Planar Waveguides on a Silicon on Insulator Platform," *International Journal of Engineering and Technology*, vol. 2, pp. 245-251, 2010.

[14] M. Bachmann, P. A. Besse, and H. Melchior, "General self-imaging properties in N x N multimode interference couplers including phase relations," *Applied Optics*, vol. 33, pp. 3905-, 1994.

[15] L. B. Soldano and E. C. M. Pennings, "Optical multi-mode interference devices based on self-imaging :principles and applications," *IEEE Journal of Lightwave Technology*, vol. 13, pp. 615-627, Apr 1995.

[16] W. P. Huang, C. L. Xu, W. Lui, and K. Yokoyama, "The perfectly matched layer (PML) boundary condition for the beam propagation method," *IEEE Photonics Technology Letters*, vol. 8, pp. 649 - 651, 1996.

[17] J. M. Heaton and R. M. Jenkins, " General matrix theory of self-imaging in multimode interference(MMI) couplers," *IEEE Photonics Technology Letters*, vol. 11, pp. 212-214, 1999.

[18] K. Rao and P. Yip, *Discrete Cosine Transform: Algorithms, Advantages, Applications*: Academic Press, 2007.

[19] F. Liu, Q. Li, and Z. Z. e. al., "Optically tunable delay line in silicon microring resonator based on thermal nonlinear effect," *IEEE Journal of Selected Topics in Quantum Electronics*, vol. 14, pp. 706 - 712, 2008.

[20] Y. Vlasov and S. McNab, "Losses in single-mode silicon-on-insulator strip waveguides and bends," *Optics Express*, vol. 12, pp. 1622-1631, 2004.

[21] N. N. Feng, C. Xu, W. P. Huang, and D. G. Fang, "A new pre-conditioner based on paraxial approximation for stable and efficient reflective beam propagation method," *IEEE Journal of Lightwave Technology*, vol. 21, pp. 1996 - 2001, 2003.

[22] L. T. Thanh and L. Cahill, "The Design of 4×4 Multimode Interference Coupler Based Microring Resonators on an SOI Platform," *Journal of Telecommunications and Information Technology, Poland*, pp. 98-102, 2/2009.

[23] T. T. Le, L. W. Cahill, and D. Elton, "The Design of 2x2 SOI MMI couplers with arbitrary power coupling ratios," *Electronics Letters*, vol. 45, pp. 1118-1119, 2009.